Supporting Information

Biopolymer-gated Ionotronic Junctionless Oxide Transistor Array for Spatiotemporal Pain-perceptual Emulation in Nociceptor Network

Yanran Li[1#], Kai Yin[1#], Yu Diao[1], Mei Fang[1], Junliang Yang[1], Jian Zhang[2], Hongtao Cao[3]，Xiaoliang Liu[1]*, and Jie Jiang[1]*

[1]Hunan Key Laboratory of Nanophotonics and Devices, School of Physics and Electronics, Central South University, 932 South Lushan Road, Changsha, Hunan 410083, P. R. China.
[2]School of Material Science and Engineering, Guilin University of Electronic Technology, Guilin, 541004, P. R. China.
[3]Laboratory of Advanced Nano Materials and Devices, Ningbo Institute of Materials Technology and Engineering, Chinese Academy of Sciences, Ningbo 315201, P. R. China.
E-mail: xl_liu@csu.edu.cn; jiangjie@csu.edu.cn

#These authors contributed equally to this work.

Note S1. The mobile-ions-induced electric-double-layer (EDL) effect

The fundamental characterizations of the ion-modulated at SA/ITO interfaces can be discussed by the following mechanism. In the previous reports, the SA has been demonstrated as a proton-conducting electrolyte.[1,2] Application of a voltage to the gate electrode causes migration and accumulation of ions at the gate-electrolyte and semiconductor-electrolyte interfaces, and then equal mirror-image charges are induced at the other side of the interface as shown Fig. 1c and d. The ions at these interfaces screen the charges in the gate electrolyte and cause accumulation of carriers in the semiconductor channel.[3,4] As shown in Fig. 1c, when V_{GS} >0, the cations are electrically induced and consecutively accumulate at the SA/channel interface, which in turn causes accumulation of electrons in the channel layer to form a conductive channel through the cations/electron electrostatic coupling effect. When the V_{GS} <0, the situation is just on the contrary as shown in Fig. 1d.

Note S2. Fitting analysis of the threshold voltage (V_{th})

The relationship between EPSC (I) and voltage amplitude (U) can be well fitted by a single exponential function:

$$I=I_1 e^{\frac{U}{U_0}} + I_0 \quad \text{(S1)}$$

where I_0 and I_1 represent two different constants. Furthermore, the fitting results can be summarized from Fig. S6 to Fig. S10.

Note S3. Two-phase sensitivity phenomenon of the biological nociceptors system.

As shown in Fig.3(h), EPSC gradually grows larger as the spike number increases. This change can be qualified as two-phase. In the initial phase, EPSC increased rapidly. Then, it would response un-sharply like the previous stage after it approaches/exceeds the threshold current level. Based on this point, it is clearly observed that the two-phase sensitivity phenomenon of the biological nociceptors system can be mimic for our device. The above experimental data can be well fitted by using a double-exponential equation:

$$K = Q_1 e\frac{-t}{q_1} + Q_2 e\frac{-t}{q_2} + K_1 \quad \text{(S2)}$$

where K_1 is EPSC constant, the Q_1 and Q_2 are original facilitation magnitudes of the two phases, and the q_1 and q_2 are respective characteristic response times of the two phases. The specific fitting results of these parameters are summarized in Table S2. From this table, we

found that q_1 is greater than the q_2. Moreover, they can be well fitted with the following equation:

$$q_1 = r_1 U + r_0 \tag{S3}$$

where r_1 and r_0 are the slope factor and initial value of the q_1-U relationship curve, respectively. Fitting the data to Equation (S3) yields r_1 and r_0 of 0.027s/V and 0.008s, respectively. The q_2-U relationship can be also fitted using the following equation:

$$q_2 = r_3 U + r_2 \tag{S4}$$

where r_3 and r_2 are the slope factor and initial value of the q_2-U relationship curve, respectively. Fitting the data to Equation (S4) yields r_3 and r_2 of 0.380s/V and 0.078s, respectively. The small time of first phase of sensitivity phenomenon in biological nociceptors system can be attributed to the protonic higher mobility and fast relaxation.[3-4] Nevertheless, with the stimulus time becomes larger, low mobility and slow relaxation of protons in sodium alginate bio-polymer electrolyte would occur, thus resulting to the slow phase with a large time constant. More interestingly, the value of q_1 and q_2 gradually grows larger as the voltage increases as shown the Table S3. This phenomenon can be attributed to electric double layer (EDL) modulation due to the residual ions at the SA/ITO interface.[1,2] Further increase in the amplitude leads to a larger output current and accordingly the time required to restore equilibrium position would increase, corresponding to a stronger harmful stimulus.[5,6] It is to be noted that, the r_3 is greater than r_1, which implies that tuning the spike amplitude has a greater impact on q_2 than q_1.

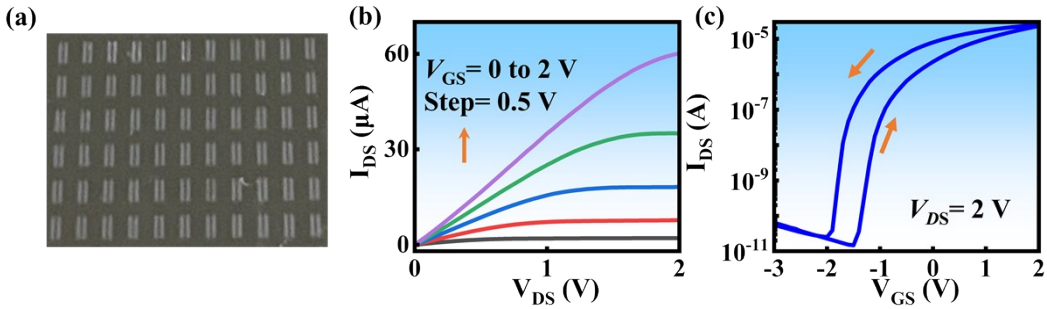

Supplementary Fig. S1. (a) The optical images of ITO devices. (b) The output curve of the ITO transistor. (c) The corresponding transfer curve of the ITO transistor with a fixed bias of V_{DS} = 2 V.

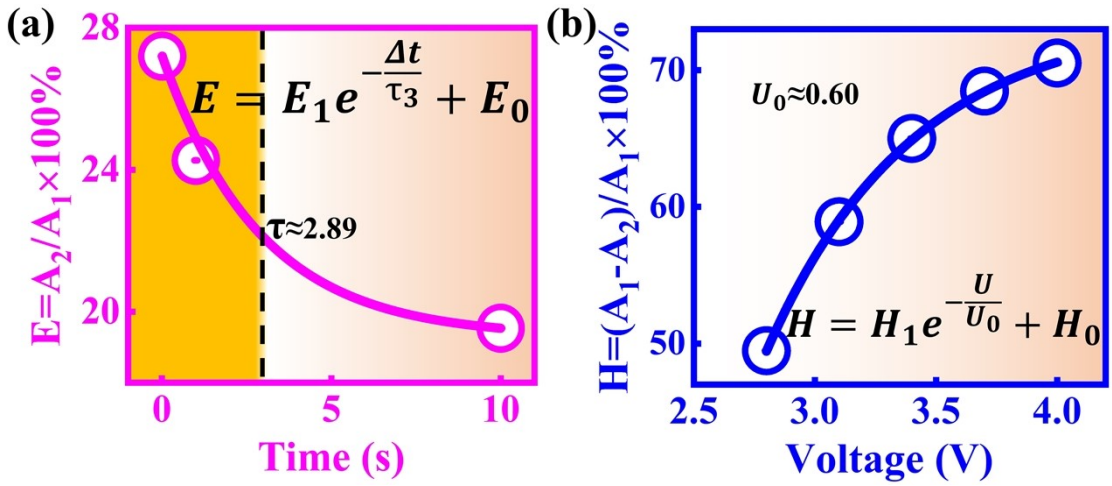

Supplementary Fig. S2. (a) The *E* index is a function of the time interval (*Δt*) between two continuous. (b) The *H* index plotted as a function of electrical spiking voltage amplitude of the first stimulus train.

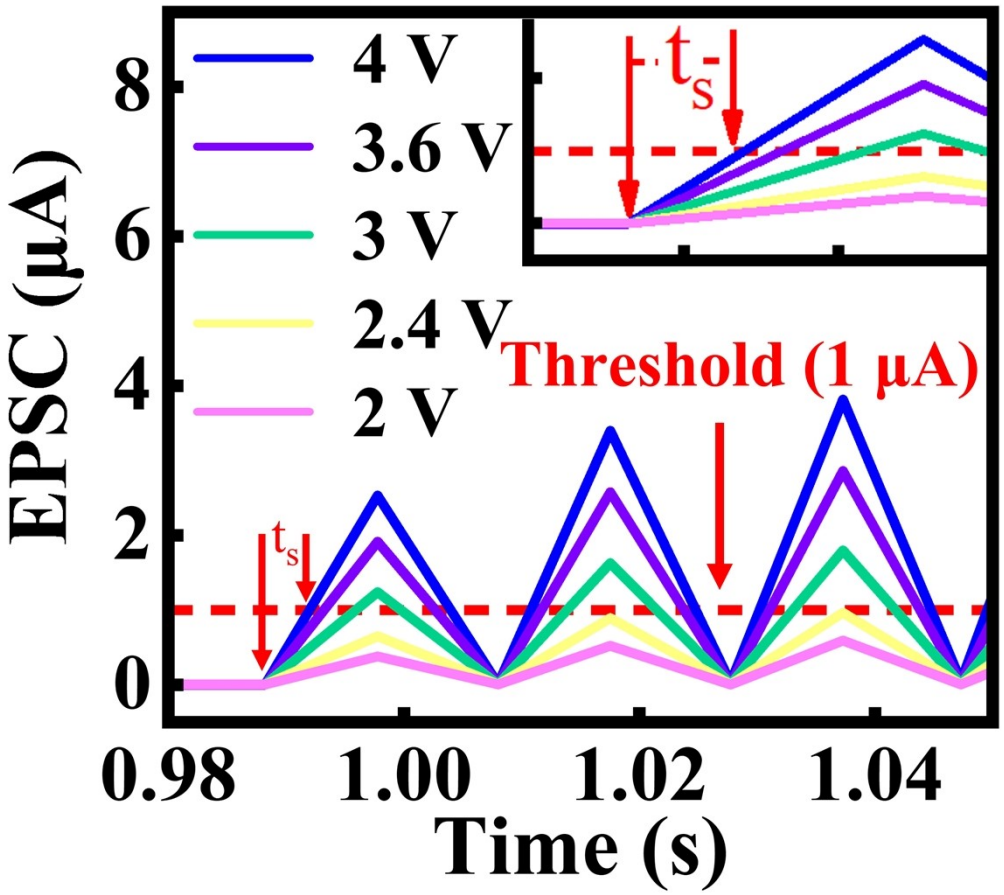

Supplementary Fig. S3. A local zoom view of Fig. 3(h). Inset: a local zoom view of S3.

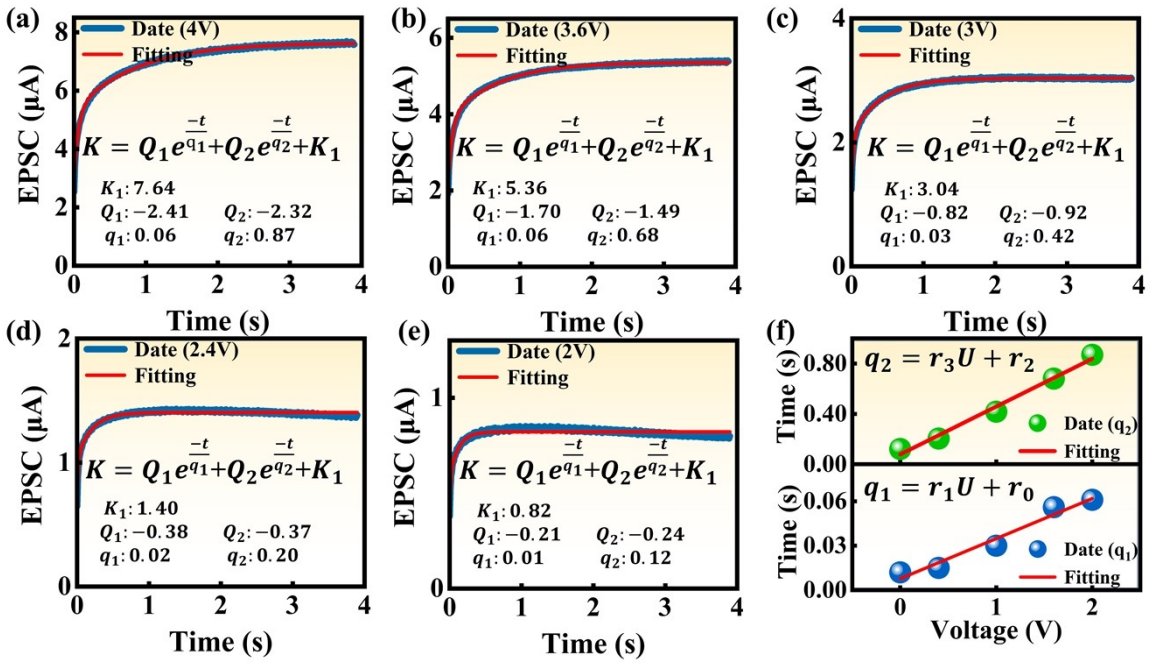

Supplementary Fig. S4. The fitting for EPSC of device to continuous multiple pulses with 4 V (a), 3.6 V (b), 3 V (c), 2.4 V (d), and 2 V (e), respectively. (f) The first stage of two-phase sensitivity (q_1) and the second stage of two-phase sensitivity (q_2) as two functions of the electric amplitude.

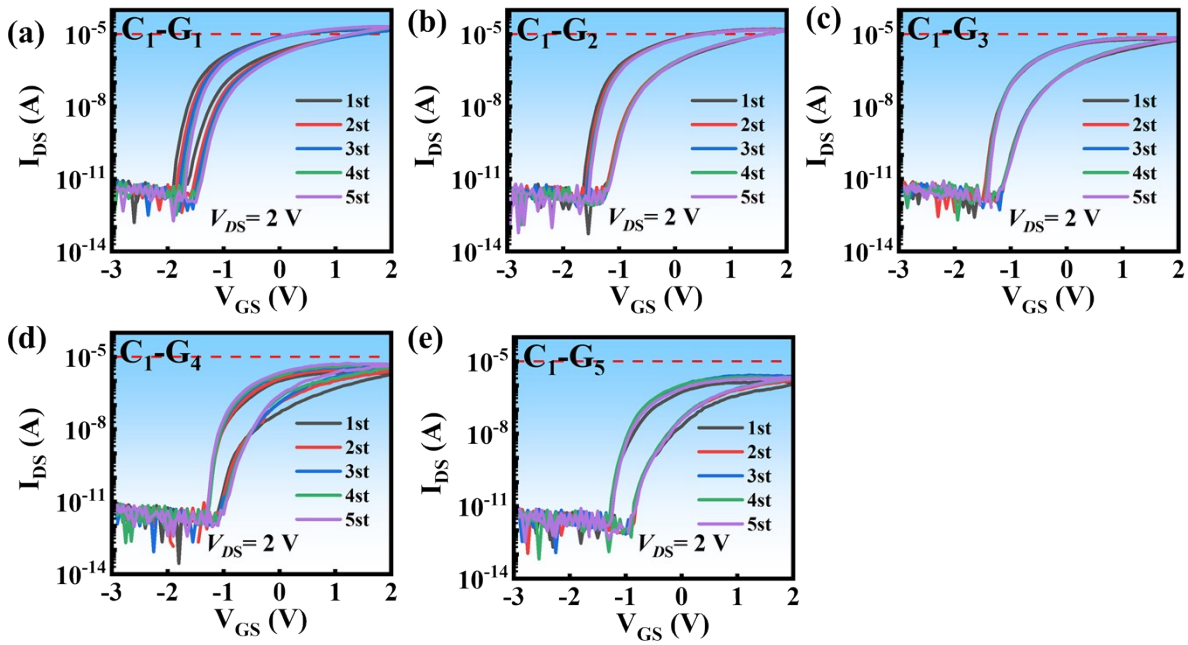

Supplementary Fig. S5. The transfer curve of Channel 1 is modulated by different gate terminals (G_1~G_5) under the fixed bias of VDS=2V for five successive measurements. (a) Modulated by G_1; (b) Modulated by G_2; (c) Modulated by G_3; (d) Modulated by G_4; (e) Modulated by G_5.

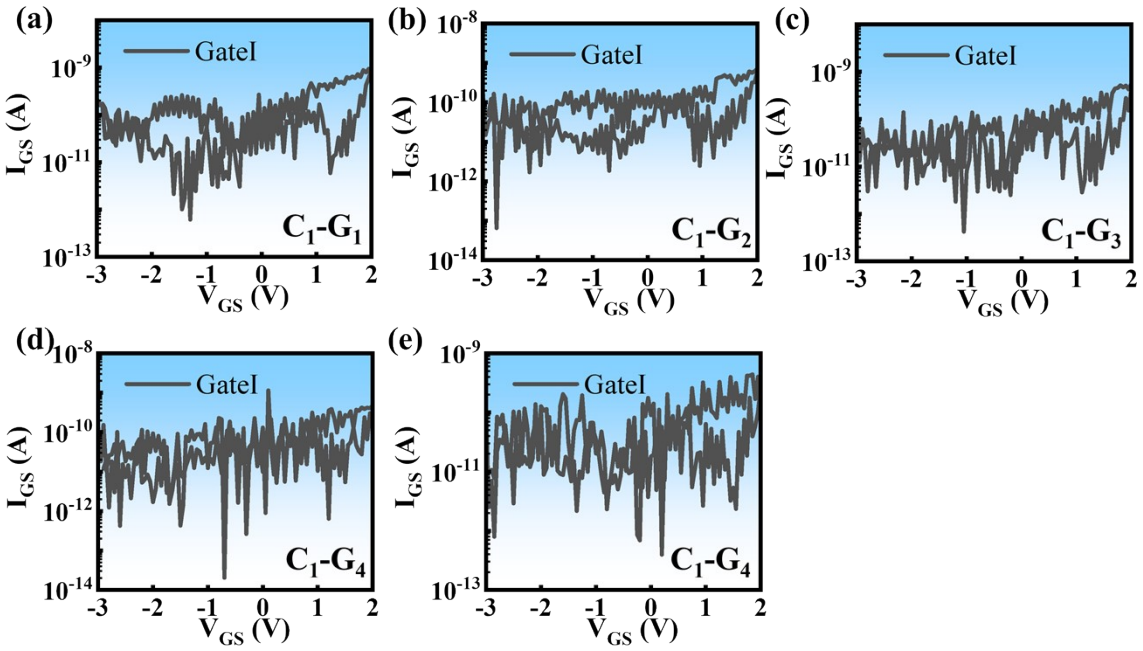

Supplementary Fig. S6. The transfer curve of Channel 1 is modulated by different gate terminals (G_1~G_5) under the fixed bias of VDS=2V for five successive measurements. (a) Modulated by G_1; (b) Modulated by G_2; (c) Modulated by G_3; (d) Modulated by G_4; (e) Modulated by G_5.

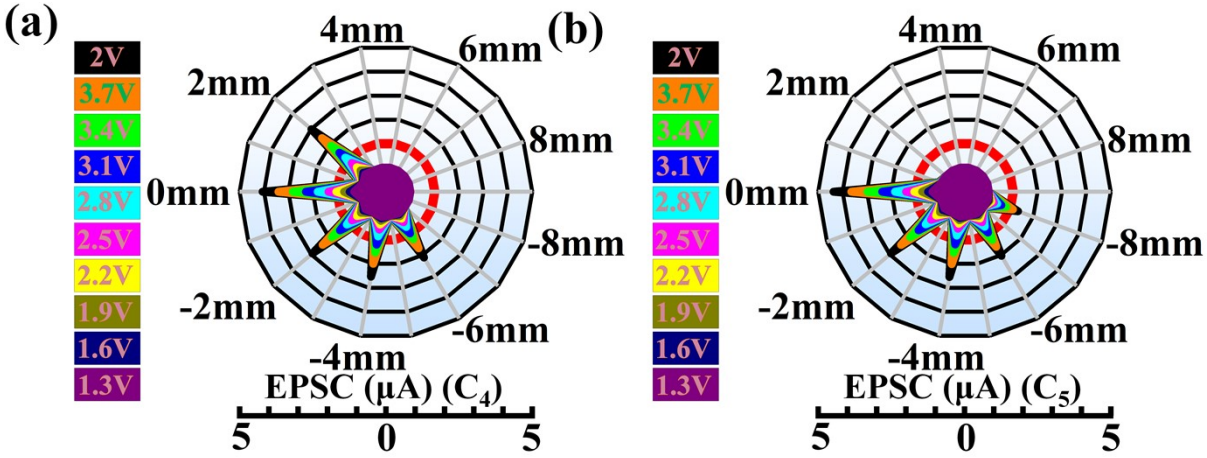

Supplementary Fig. S7. (a) The EPSC responses with different projection for Chan-4. (b) The EPSC responses with different projection for Chan-5.

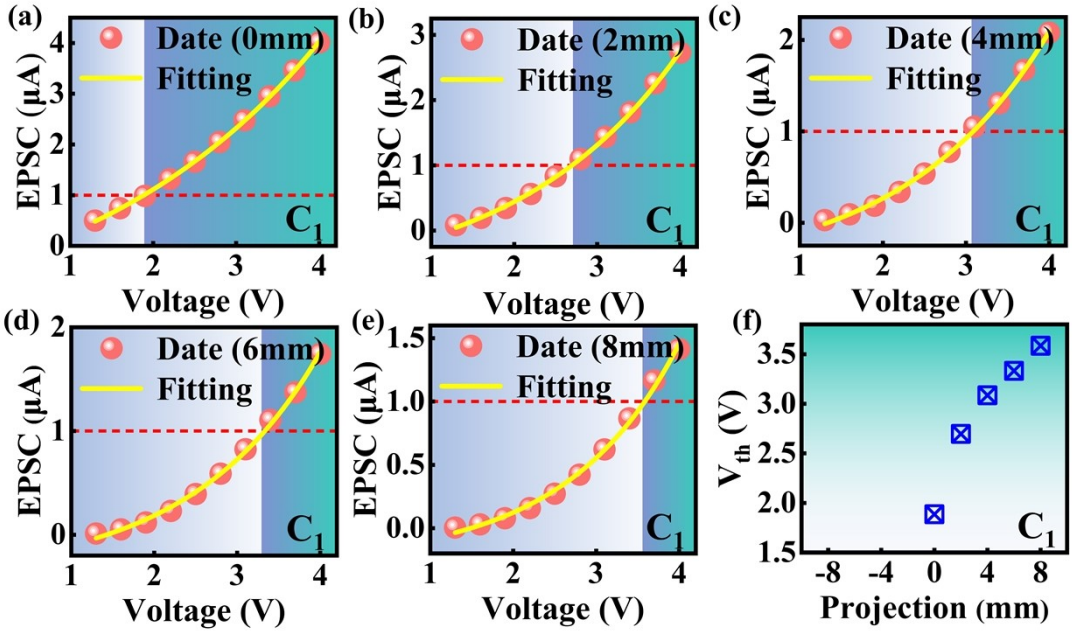

Supplementary Fig. S8. EPSC of Chan-1 as a function of voltage under a fixed projection of 0mm (a), 2mm (b), 4mm (c), 6mm (d), and 8mm (e), respectively. (f) The corresponding value of V_{th} is concluded by Equation (S1).

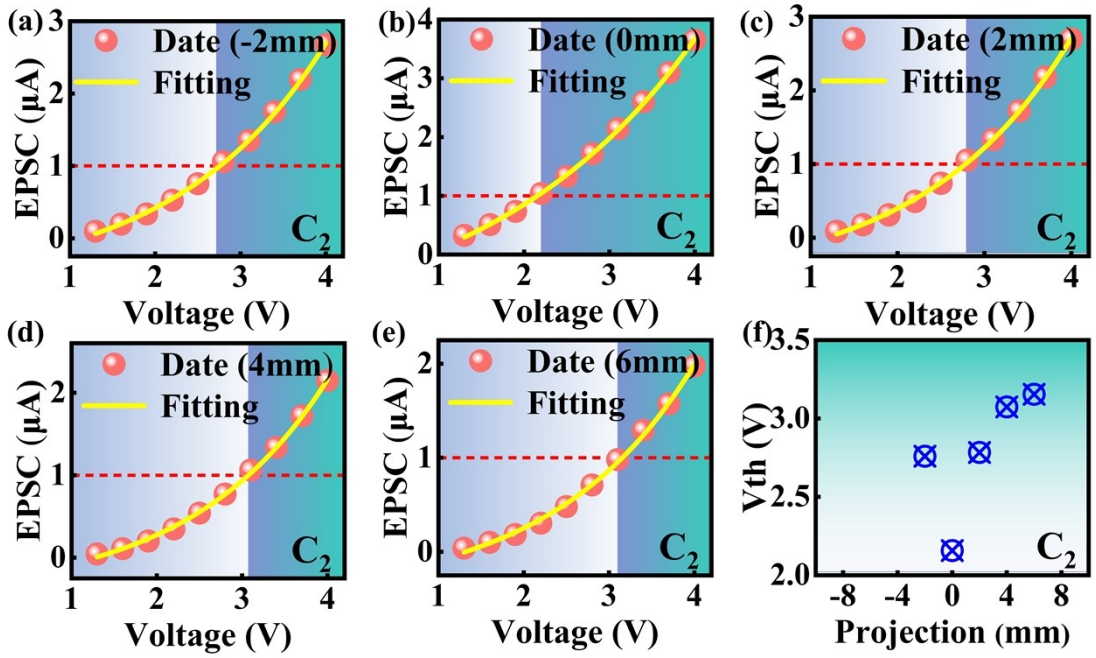

Supplementary Fig. S9. EPSC of Chan-2 as a function of voltage under a fixed projection of -2mm (a), 0mm (b), 2mm (c), 4mm (d), and 6mm (e), respectively. (f) The corresponding value of V_{th} is concluded by Equation (S1).

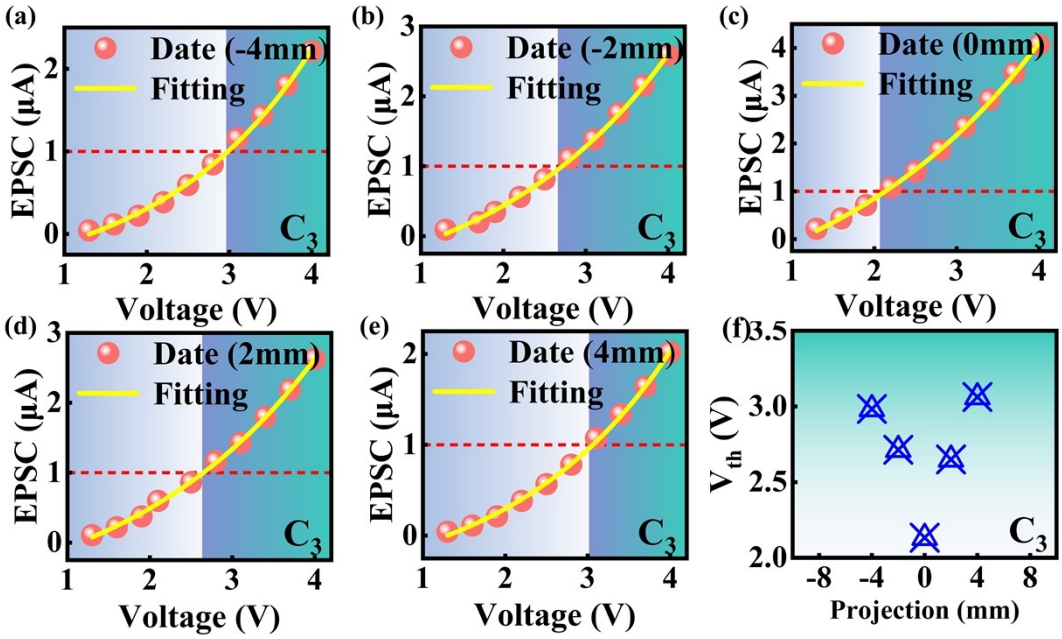

Supplementary Fig. S10. EPSC of Chan-3 as a function of voltage under a fixed projection of -4mm (a), -2mm (b), 0mm (c), 2mm (d), and 4mm (e), respectively. (f) The corresponding value of V_{th} is concluded by Equation (S1).

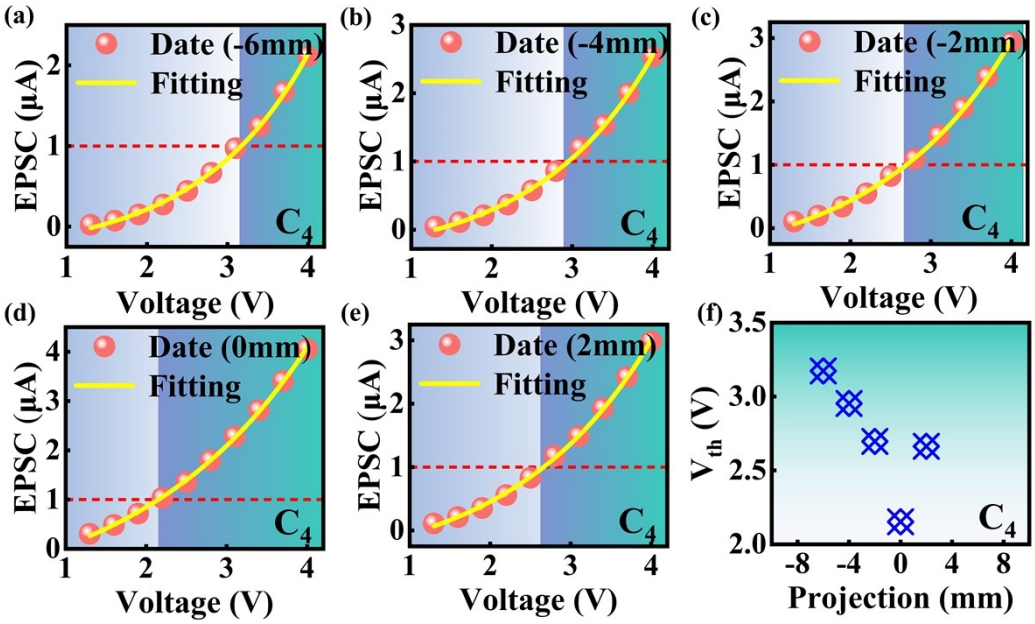

Supplementary Fig. S11. EPSC of Chan-4 as a function of voltage under a fixed projection of -6mm (a), -4mm (b), -2mm (c), 0mm (d), and 2mm (e), respectively. (f) The corresponding value of V_{th} is concluded by Equation (S1).

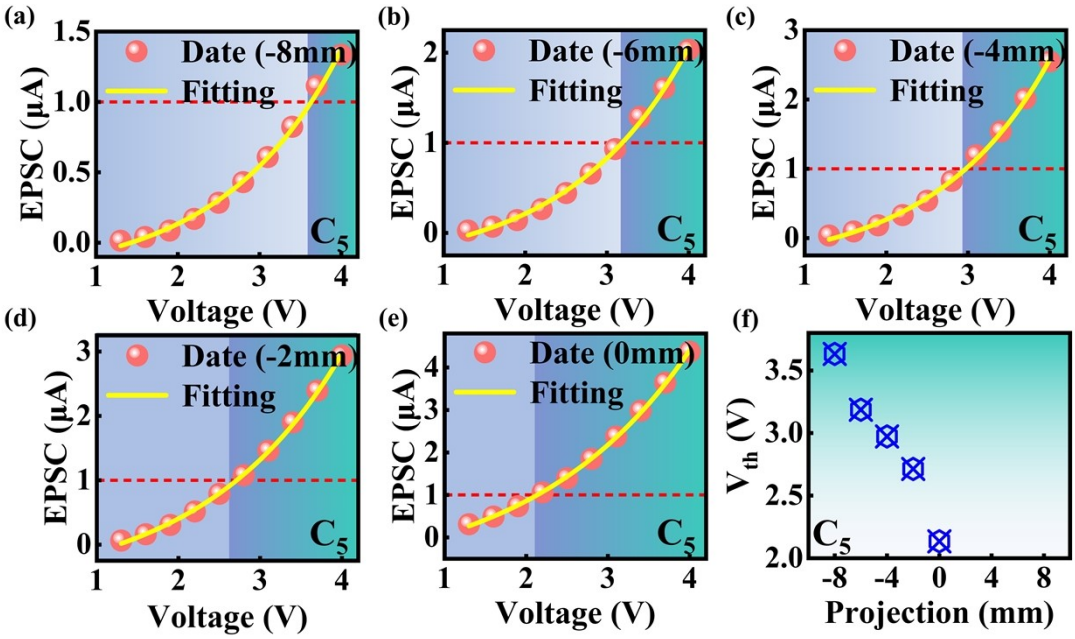

Supplementary Fig. S12. EPSC of Chan-5 as a function of voltage under a fixed projection of -8mm (a), -6mm (b), -4mm (c), -2mm (d), and 0mm (e), respectively. (f) The corresponding value of V_{th} is concluded by Equation (S1).

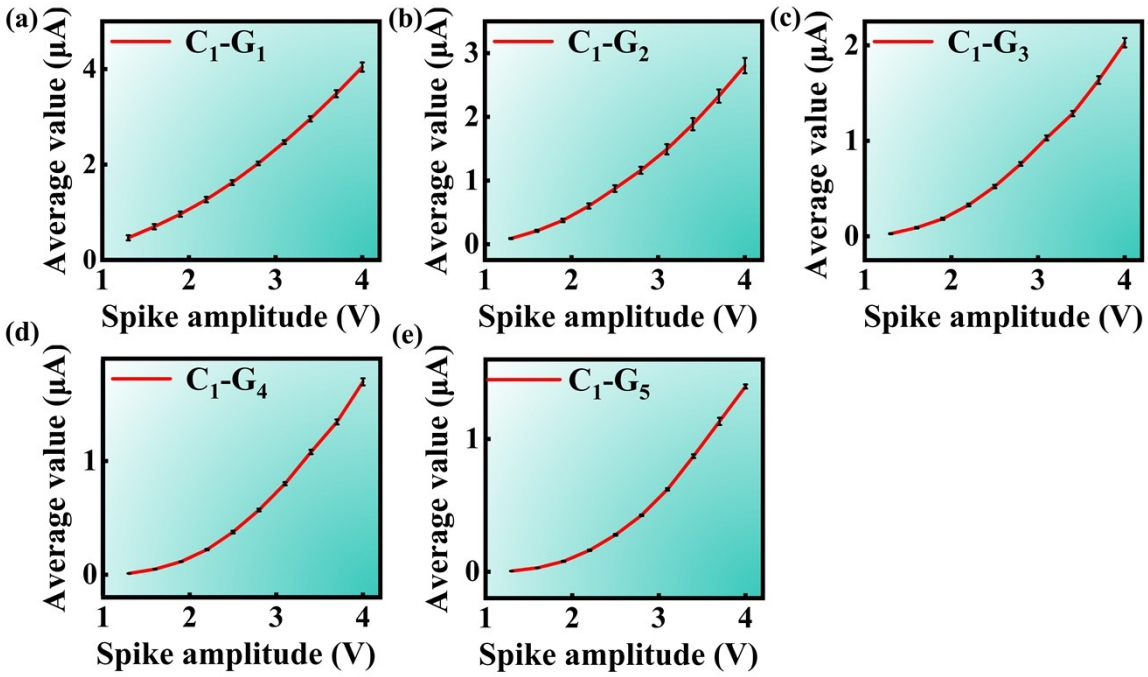

Supplementary Fig. S13. The stability of oxide transistor is demonstrated by measuring the EPSC for five successive measurements. (a) The stability of Chan-1 with Gate 1. (b) The stability of Chan-1 with Gate 2. (c) The stability of Chan-1 with Gate 3. (d) The stability of Chan-1 with Gate 4. (e) The stability of Chan-1 with Gate 5.

E_1	E_0	τ_3(s)	H_1	H_0	U_0 (V)
7.94	19.29	2.89	-2559.60	73.92	0.60

Supplementary Table S1. The fitting results for the different parameters are summarized from Fig. S2.

Spiking amplitudes (V)	Incubation time (ms)
4	3
3.6	5
3	7
2.4	68
2	>7000

Supplementary Table S2. The incubation time corresponding to different voltage amplitudes.

Voltage (V)	K_1	Q_1	Q_2	q_1 (s)	q_2 (s)
4.0	7.64	-2.41	-2.32	0.06	0.87
3.6	5.36	-1.70	-1.49	0.06	0.68
3.0	3.04	-0.82	-0.92	0.03	0.42
2.4	1.40	-0.38	-0.37	0.02	0.20
2	0.82	-0.21	-0.24	0.01	0.12

Supplementary Table S3. The summarized table of the fitting results (K_1, Q_1, Q_2, q_1 and q_2) for two-phase sensitivity.

	Chan-1	Chan-2	Chan-3	Chan-4	Chan-5
Gate 1	0	-2	-4	-6	-8
Gate 2	2	0	-2	-4	-6
Gate 3	4	2	0	-2	-4
Gate 4	6	4	2	0	-2
Gate 5	8	6	4	2	0

Supplementary Table S4. The value of the projection formed between the different channels and gates.

References

1 G. Feng, J. Jiang, Y. Zhao, S. Wang, B. Liu, K. Yin, *Adv. Mater.*, 2020, **32**, 1906171.
2 G. Feng, J. Jiang, Y. Li, D. Xie, B. Tian, Q. Wan, *Adv. Funct. Mater.*, 2021, **31**, 2104327.
3 Z. Zheng, J. Jiang, J. Guo, J.Sun, J. Yang, *Organic Electronics*, 2016, **33**, 311-315.
4 W. Hu, J. Jiang, D. Xie, S. Wang, K. Bi, H. Duan, J.Yang, Jun He, *Nanoscale*, 2018, **10**, 14893–14901.
5 H. Ikeda, J. Stark, H. Fischer, M. Wagner, R. Drdla, T. Ja¨ger, Synaptic Amplifier of Inflammatory Pain in the Spinal Dorsal Horn. *Science* 2006, **312**, 1659-1662.
6 M. C. Acosta, C. Luna, S. Quirce, C. Belmonte, J. Gallar, Invest. Oph-thalmol. Vis. *Sci.* 2014, **5**, 3403-3412.